

## Supplementary Information to the manuscript

### Saxitoxin and tetrodotoxin bioavailability increases in future oceans

Roggatz, C.C.<sup>1,2\*</sup>, Fletcher, N.<sup>2</sup>, Benoit, D.M.<sup>3</sup>, Algar, A.C.<sup>4</sup>, Doroff, A.<sup>5</sup>, Wright, B.<sup>6</sup>, Wollenberg Valero, K.C.<sup>2</sup>, and Hardege, J.D.<sup>2</sup>

\*Corresponding author: C.Roggatz@hull.ac.uk

#### Supplementary Methods

##### **Biotoxin charge distribution models including explicit solvation**

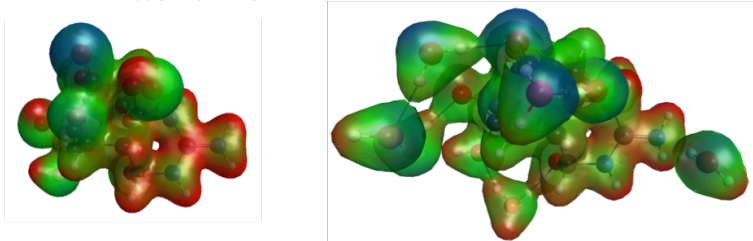
The properties of molecules in solution are partly influenced by the water molecules surrounding them and the direct interactions between the solute and the solvent molecules. We therefore wanted to ensure that surrounding water molecules do not significantly affect the changes in charge distribution observed with protonation of both toxin molecules and so potentially counterbalance the effect of pH on their toxicity. We added one water molecule per ionisable group to the optimised conformers of tetrodotoxin (TTX) and saxitoxin (STX), as we found this to be a representative ratio in previous work<sup>1</sup>, and performed a second full cycle of optimisation as described in the method section of the main paper. The charge distribution was calculated using the PBE0 exchange correlation functional<sup>2</sup> in conjunction with a STO-3G basis set<sup>3,4</sup> and the visualisation was performed with the same parameters described for the models without explicit water molecules. To ensure the choice of basis set did not influence the results significantly, the partly protonated form of STX (STX<sup>+</sup>) was calculated using the STO-3G as well as the pc-2 basis set. The latter had been used initially to calculate the charge distribution of the models without explicit water, but is much more computationally costly.

#### Supplementary Results

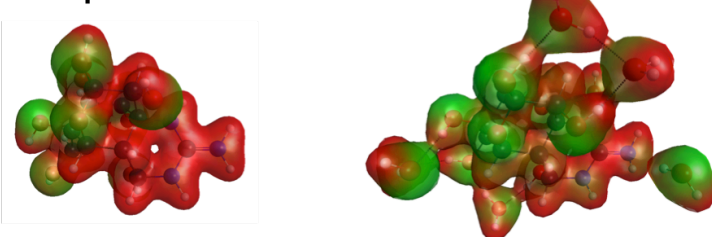
##### **Biotoxin charge distribution models including explicit solvation**

Additional water molecules were found to not level out the charge differences across both toxin molecules, which is shown in Supplementary Fig. S1 (left compared to right). The charge differences between protonation states were also present when explicit water molecules were added. Using a smaller basis set (STO-3G) was not found to influence results compared to the larger basis set (pc-2). It needs to be noted that not all pH effects on the charge distribution are “bad”: decreasing pH protonates the –SH cysteine and imidazole ring side chains of histidine residues in the selectivity region of the ion channel, causing a faster rate of recovery from receptor blockage<sup>5,6</sup> although it is unknown which relevance this may have.

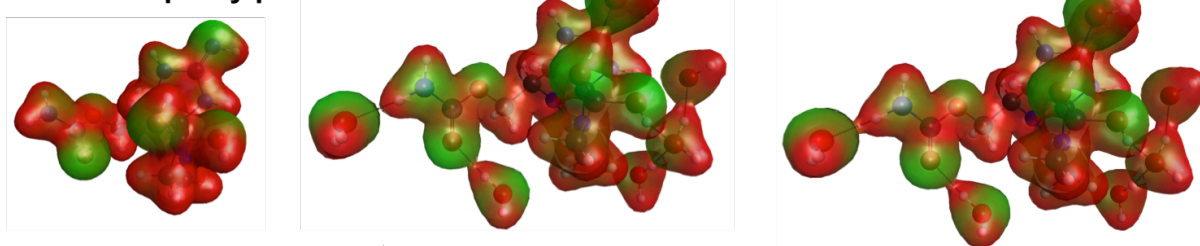
**a TTX<sup>0</sup> – zwitterion form**



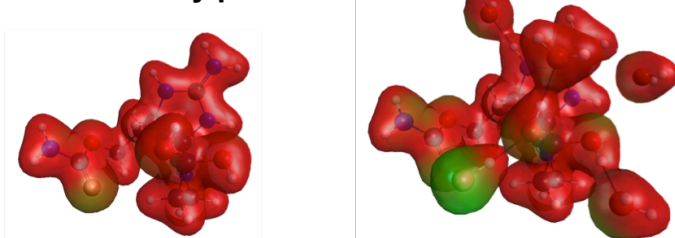
**b TTX<sup>+</sup> – protonated form**



**c STX<sup>+</sup> – partly protonated form**



**d STX<sup>2+</sup> – fully protonated form**



**Supplementary Fig. S1. Charge distribution around computationally optimised conformations (PBE0/pc-2) of tetrodotoxin (TTX, a & b) and saxitoxin (STX, c & d) using different solvation models.** On the left, the conformers optimised using the COSMO implicit solvation model are shown. The charge distribution for visualisation was calculated at the PBE0/pc-2 level of theory. In the middle, the conformers optimised in a cluster with one water molecule per ionisable group in addition to implicit solvation (COSMO) are shown. The charge distribution was calculated at the PBE0/STO-3G level of theory and exemplarily for comparison at the PBE0/pc-2 level of theory for STX<sup>+</sup> (right). The conformers of the non- or partly protonated forms (a: TTX<sup>0</sup> and c: STX<sup>+</sup>) and fully protonated forms (b: TTX<sup>+</sup> and d: STX<sup>2+</sup>) are shown with electron density iso-surfaces coloured based on the electrostatic potential. Blue indicates negative, green neutral and red positive charge (see Supplementary Information for details).

### Changes in protonation state abundance of the toxic forms of other STX derivatives

PSP is often linked to a range of toxin molecules that are related to STX, but slightly chemically modified. However, they all share the 7,8,9-guanidinium group associated with the toxins' mode of action, blocking ion channels in nerves and muscles and ultimately causing paralysis. Besides STX and the exemplary derivatives dcSTX and neoSTX named in Table 1, the toxin profile of *Alexandrium sp.* and *Gymnodinium sp.* contains gonyautoxins (GTXs). For these GTX derivatives no experimental  $pK_a$  data is available. Therefore, we calculated the likely  $pK_a$  values based on the respective molecular structure using the ChemAxon Chemicalize web application (<https://chemicalize.com/>). We then calculated the changes in abundance of the toxic protonation states (those with a protonated 7,8,9-guanidinium group) for the same change in pH as in Table 1. Temperature changes could not be included since the calculated  $pK_a$  data is not temperature-referenced. GTX 1 & 4 as well as 2 & 3 only differ stereochemically in the  $OSO_3^-$  group, which is unlikely to affect the  $pK_a$  constants. They therefore can be assumed to have the same abundance curves of protonation states. All six GTX derivatives show a clear increase in the abundance of the toxic forms (see Supplementary Table 1).

**Supplementary Table 1:** Change in abundance of GTX1 to 6 in future oceanic pH.

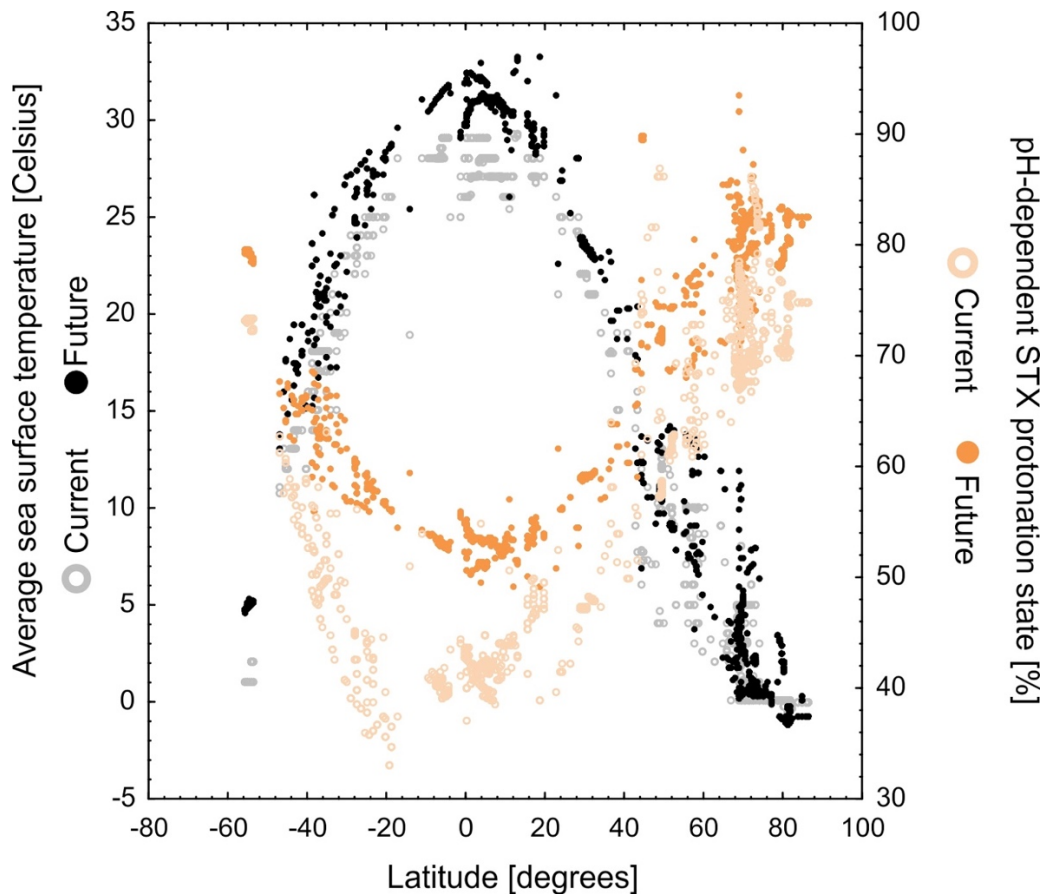
Compound	Change in abundance of toxic form(s) protonated at the 7,8,9-guanidinium group	
	pH 8.1 → pH 7.7	pH 8.1 → pH 7.2
GTX <sub>1,4</sub>	+ 17.8%	+ 29.3%
GTX <sub>2,3</sub>	+ 24.8%	+ 48.2%
GTX <sub>5</sub>	+ 23.3%	+ 53.9%
GTX <sub>6</sub>	+ 19.5%	+ 32.7%

Note: These changes do not include effects of temperature.

### **Interpolation maps for spatial prediction of protonation state**

In total, three interpolation maps were generated: These included (i) STX protonation levels at current pH and current mean SST; (ii) STX protonation levels computed from future pH under the RCP8.5 model (2045-2101) and CMIP3 future predicted SST (2087-2096); (iii) the absolute difference between current and future (RCP8.5) predicted protonation levels (see Figure 2). Standard errors of Kernel interpolation models ranged between 0.15 and 13.15% and average standard errors for protonation state or their differences for each map were (i) 2.66%, (ii) 2.41%, and (iii) 2.45%. While current pH is higher in higher latitudes, the effect of cold temperature is likewise important in generating the spatial pattern of STX protonation which increases in colder temperatures (Fig. 2b, c). The Gulf of St. Lawrence, where harmful algal blooms (HABs) are frequent (<http://haedat.iode.org>), shows high STX bioavailability due to high freshwater influx from the St. Lawrence river, combined with the higher latitude. This pattern also extends to the North-Eastern United States where the current pH levels in Northern Maine are modelled at 7.5 and have been measured at 7.75<sup>7</sup>. Noteworthy areas of currently high and future even higher protonation levels include the Eurasian coastline of the Arctic Circle where the Bering, Barents and Kara seas (Fig. 2c) comprise pockets of very high potential STX toxicity due to extremely low pH in Northern Winter<sup>8</sup> combined with warmer temperatures. Likewise, there is a pocket of high estimated current STX toxicity along the Canadian and US West Coasts from the Bering strait to Vancouver Island, aligning with a multitude of recorded HABs in that area. However, the future model predicts that this pocket will be significantly extended towards California (Fig 2c). It needs to be discussed that STX in current oceanic conditions is always at least 26% protonated, which can also help to explain the occurrence of PSP-related HABs in areas which have the current lowest values of STX toxicity such as the UK<sup>9</sup>. Lastly, we have to point out that different from the present pH raster we used (Fig. 2a), the future predictions (Fig. 2b) did not include freshwater influx nor upwelling events; which is why some areas with current high STX toxicity (Gulf of Lawrence) are modelled as reduced in STX protonation state in the future (Fig. 2c).

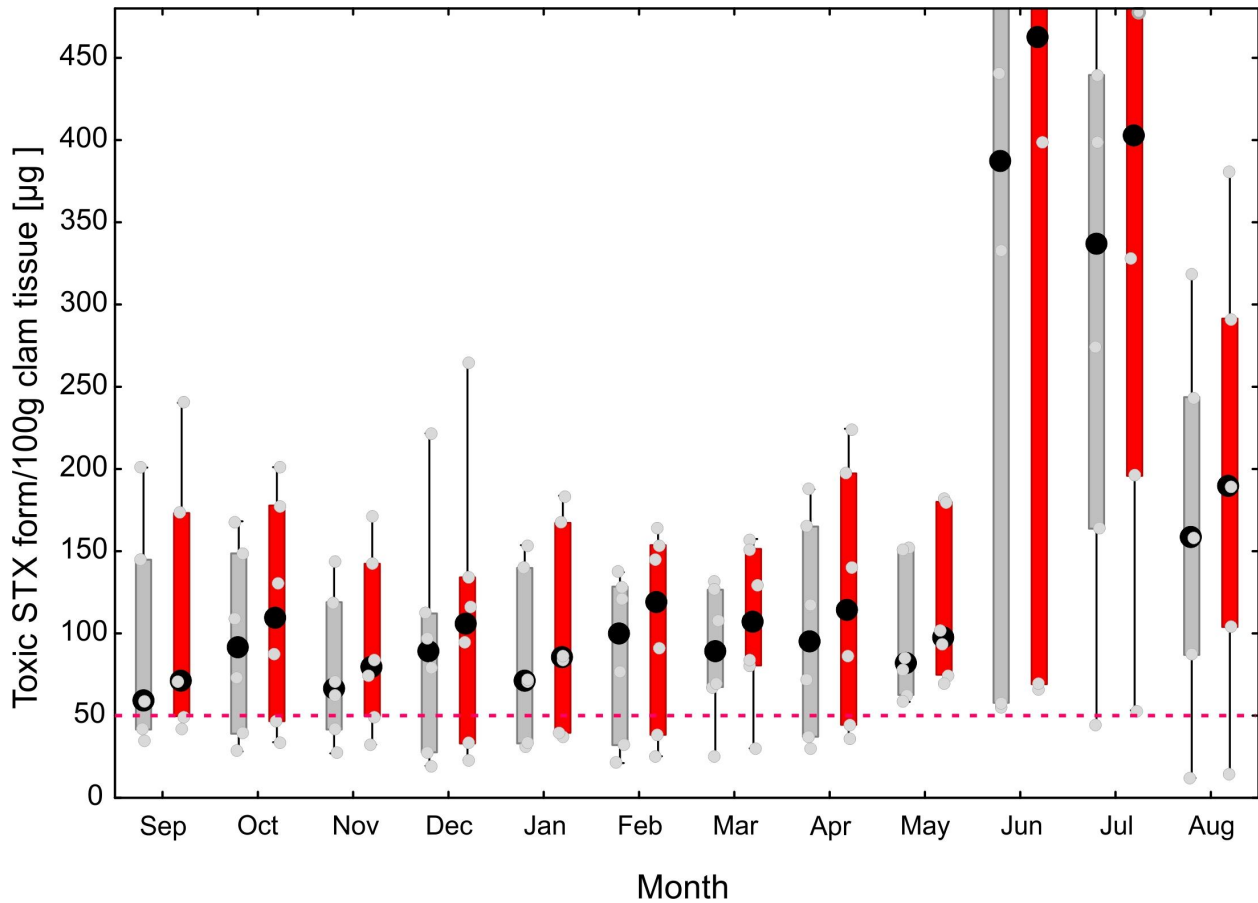
To illustrate the relationship between temperature, toxicity and latitude, we plotted the respective data for each location in Supplementary Fig. S2. This clearly shows a wide temperature range and a large range of toxicity, which increases in a location-specific manner in future conditions.



**Supplementary Fig. S2: Distribution of temperature data and toxic STX abundance data with respect to latitude based on the points used for the spatial interpolation maps in Fig. 2.** Data for current conditions at each location is shown by open circles, data for conditions in the year 2100 according to the RCP 8.5 scenario (Future) as filled circles. Average sea surface temperature ranges between -1 and 33°C (grey/ black circles, legend on the left) and abundance of the toxic protonated state ranges from 32 to 94% (orange circles, legend on the right).

### Seasonal variability of STX content in butter clam tissue

To illustrate the extent of seasonal variability, the saxitoxin content in clam tissue was further averaged for each month based on the data obtained for the time frame between June 2012 and July 2018. Results are shown below in Supplementary Fig. S3. Values in May, June, July and August frequently exceed the FDA limit with toxic STX content, being especially high in June and July. Focussing on the red bars also shows that in future the critical toxic STX content will also be more frequently exceeded in spring and autumn, extending the critical time period in which consumption cannot be deemed safe and lead to paralytic shellfish poisoning.



**Supplementary Fig. S3. Seasonality of the amount of the toxic saxitoxin state present in 100g butter clam *Saxidomus gigantea* tissue at Sand Point's Spit Beach, Alaska** (n= 6 years with 73 monthly data points). June values are displayed up to 480  $\mu\text{g}/100\text{ g}$  and data range to 6,580  $\mu\text{g}/100\text{ g}$ . Toxic STX content based on today's conditions from the map projection in Fig. 2a is coloured in grey, amount of toxic STX in future conditions (based on the same amount of overall toxin) are shown in red for an RCP 8.5 scenario. The pink dashed line indicates current US Food and Drug Administration (FDA) limit of 80  $\mu\text{g}/100\text{ g}$ , which equals 50.4  $\mu\text{g}/100\text{ g}$  of the toxic STX form (under current pH and temperature conditions) in seafood tissue.

## References (Supplementary Information only)

1. Roggatz, C. C., Lorch, M. & Benoit, D. M. Influence of solvent representation on nuclear shielding calculations of protonation states of small biological molecules. *J. Chem. Theory Comput.* **14**, 2684–2695 (2018).
2. Adamo, C. & Barone, V. Toward reliable density functional methods without adjustable parameters: The PBE0 model. *J. Chem. Phys.* **110**, 6158–6170 (1999).
3. Hehre, W. J., Ditchfield, R., Stewart, R. F. & Pople, J. A. Self-consistent molecular orbital methods. IV. Use of Gaussian expansions of Slater-type orbitals. Extension to second-row molecules. *J. Chem. Phys.* **52**, 2769–2773 (1970).
4. Collins, J. B., von R. Schleyer, P., Binkley, J. S. & Pople, J. A. Self-consistent molecular orbital methods. XVII. Geometries and binding energies of second-row molecules. A comparison of three basis sets. *J. Chem. Phys.* **64**, 5142–5151 (1976).
5. Hegyi, B. *et al.* Tetrodotoxin blockade on canine cardiac L-type Ca<sup>2+</sup> channels depends on pH and redox potential. *Mar. Drugs* **11**, 2140–2153 (2013).
6. Ulbricht, W. & Wagner, H. H. The influence of pH on the rate of tetrodotoxin action on myelinated nerve fibres. *J. Physiol.* **252**, 185–202 (1975).
7. Marine Coastal Observing Alliance. *Estuarine Monitoring Program Summary Report.* (2014).
8. Takahashi, T. *et al.* Climatological distributions of pH, pCO<sub>2</sub>, total CO<sub>2</sub>, alkalinity, and CaCO<sub>3</sub> saturation in the global surface ocean, and temporal changes at selected locations. *Mar. Chem.* **164**, 95–125 (2014).
9. Turner, A. D. *et al.* Fatal canine intoxications linked to the presence of saxitoxins in stranded marine organisms following winter storm activity. *Toxins* **10**, (2018).